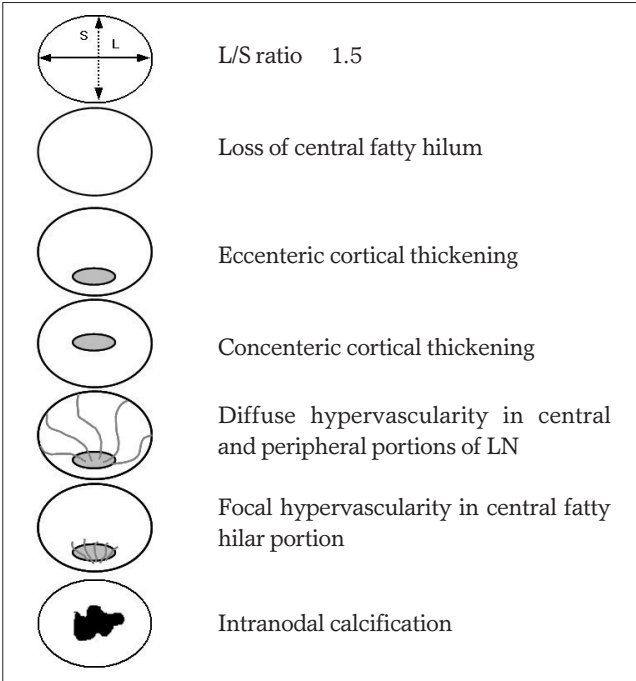




(brachial plexus) 가

(accessory breast)

(Reactive Lymphadenopathy) 가



**Fig. 1.** Sonographic features of a pathologic lymph node (LN). Pathologic LNs were differentiated from the normal nodes by the long to short axis ratio (L/S ratio), hilar echogenicity, cortical thickening, hypervascularity and intranodal calcification. LNs with L/S ratio 1.5, no hilum, and eccentric cortical thickening are suggestive of a malignancy, whereas LNs with L/S ratio >1.5, wide hilum and concentric cortical thickening are suggestive of reactive lymphadenopathy. Benign lymph nodes show focal hypervascularity in the central hilar portion, but a malignant lymphoma shows diffuse hypervascularity in the central and peripheral portions of LN.

1  
2  
3

ratio)가 1.5 (long to short axis ratio (L/S ratio))가 1.5 (eccentric cortical thickening)가 (concentric cortical thickening) (1) (2). (Tuberculous Lymphadenitis)

(collagen vascular disease), 가 가 가

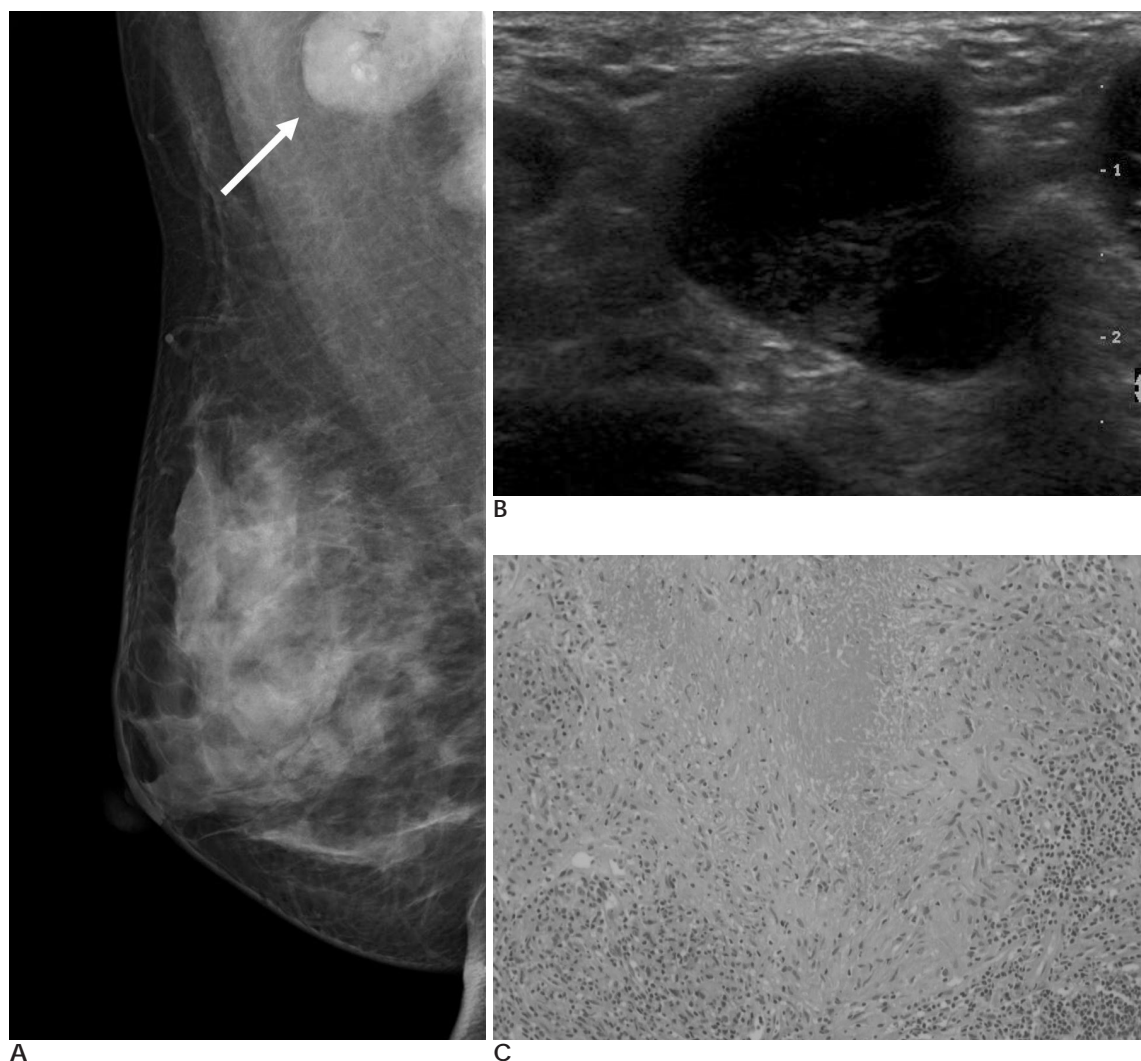


**Fig. 2.** Tuberculous lymphadenopathy in a 39-year-old female with a right axillary palpable mass. **A.** Mammogram shows multiple enlarged axillary lymph nodes with central calcifications (arrow) in the right axilla. **B.** Ultrasonography shows enlarged hypoechoic lymph node and central echogenic portion with echogenic surrounding fat due to inflammatory changes. **C.** An excisional biopsy of the right axillary masses was performed. Photomicrograph shows central caseous necrosis, epithelioid cells and multiple Langerhans-type giant cells, which are compatible with tuberculous granulomas ( $\times 40$ , H-E stain). The acid-fast organisms were positive (AFB stain, not shown).

가

(3).

가

(Dermatopathic Lymphadenitis)

(subcortical germinal center)  
( hemosiderin)가

(5).

가

가

(Fig. 4).

가  
(caseous necrosis)  
(Fig. 2).

(epithelioid cell)

Kikuchi

Kikuchi

Kikuchi

가

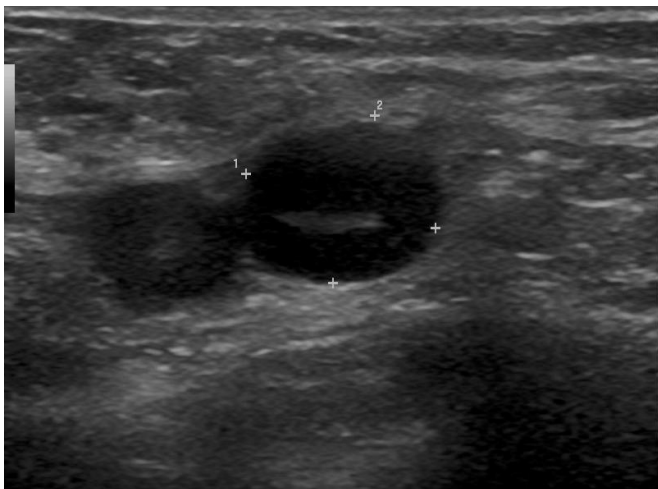
(concentric cortical thickening)

(4)

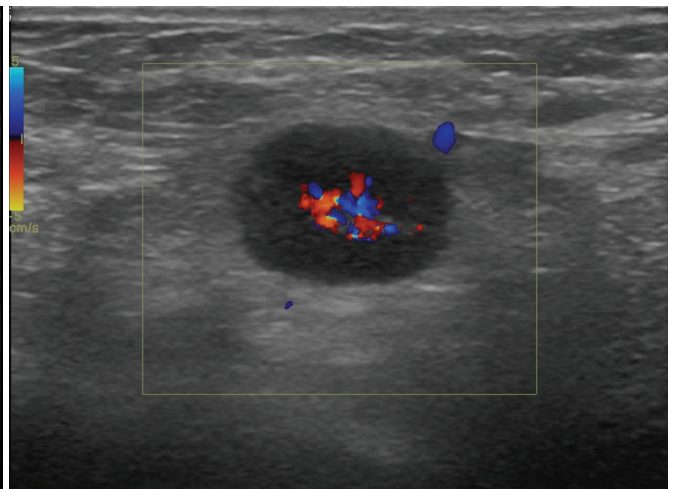
가

(Fig. 3).

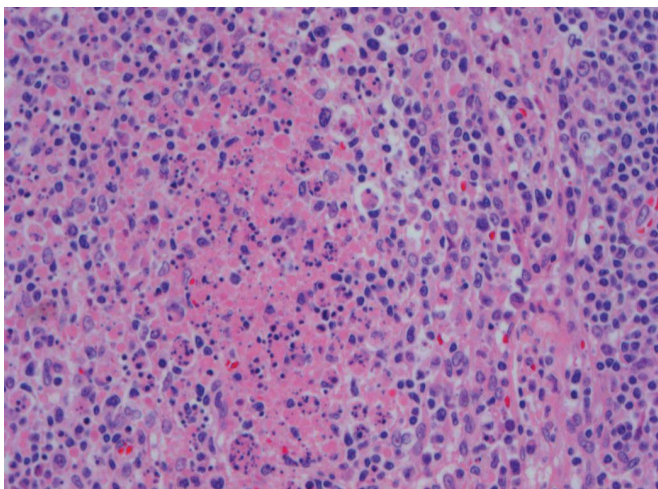
( )



A



B

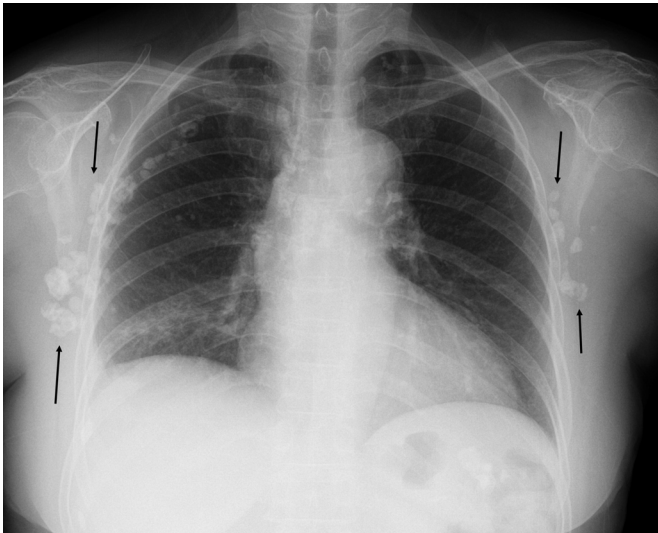


C

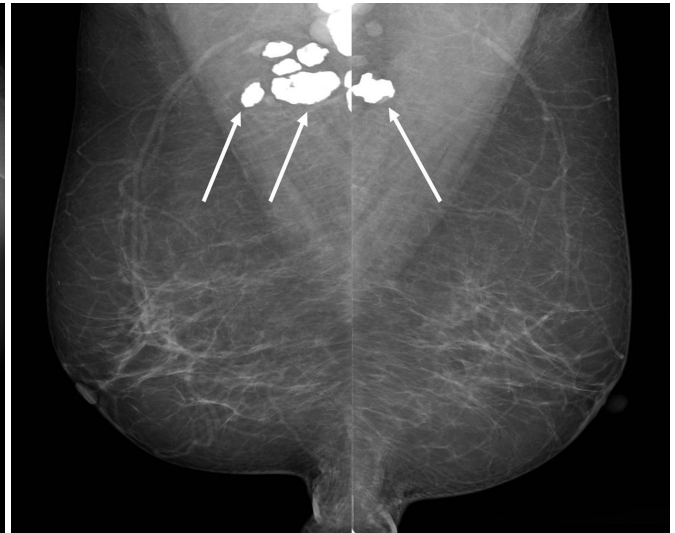
**Fig. 3.** Kikuchi's disease in a 37-year-old female at both axillae. **A, B.** Ultrasonography shows round conglomerated lymph nodes with concentric cortical thickening, but with central fatty hila remaining. The color doppler scan shows focal hypervascularity in central fatty hilar portion. **C.** Sonography-guided core biopsy was performed. Photomicrograph shows necrotic debris in Kikuchi's lymphadenopathy ( $\times 200$ , H-E stain).

가 가

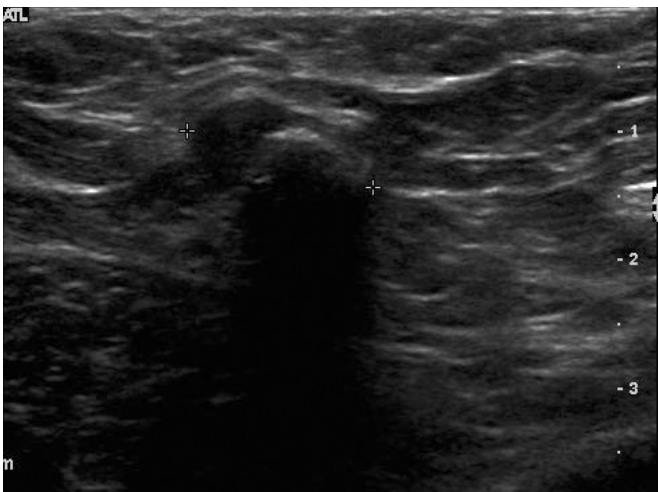
가 , , 가



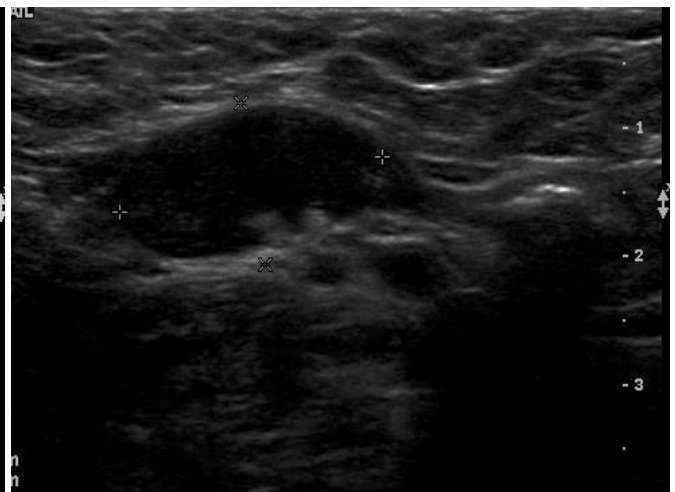
A



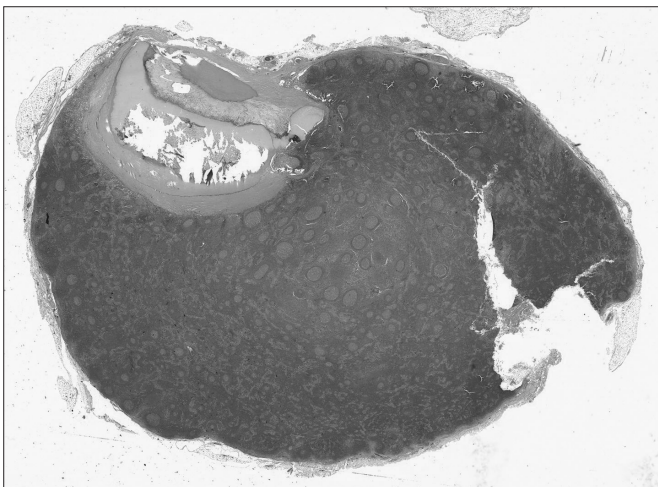
B



C



D



E

**Fig. 4.** Dermatopathic lymphadenitis in a 64-year-old female with psoriasis and both axillary masses.  
**A.** Chest PA shows multiple calcified lymph nodes located along both chest walls (arrows).  
**B.** Mammogram shows multiple dense calcified lymph nodes in both axillae (arrows).  
**C, D.** Ultrasonography reveals the multiple calcified lymph nodes to show cortical thickening with the remaining central fatty hila. The color doppler scan shows focal hypervascularity in the central fatty hilar portion of lymph node.  
**E.** An excisional biopsy of the right axillary masses was performed. Photomicrograph shows an enlarged germinal center and an enlarged paracortical center (×40, H-E stain).

가 가 가 가 가 가 가 가

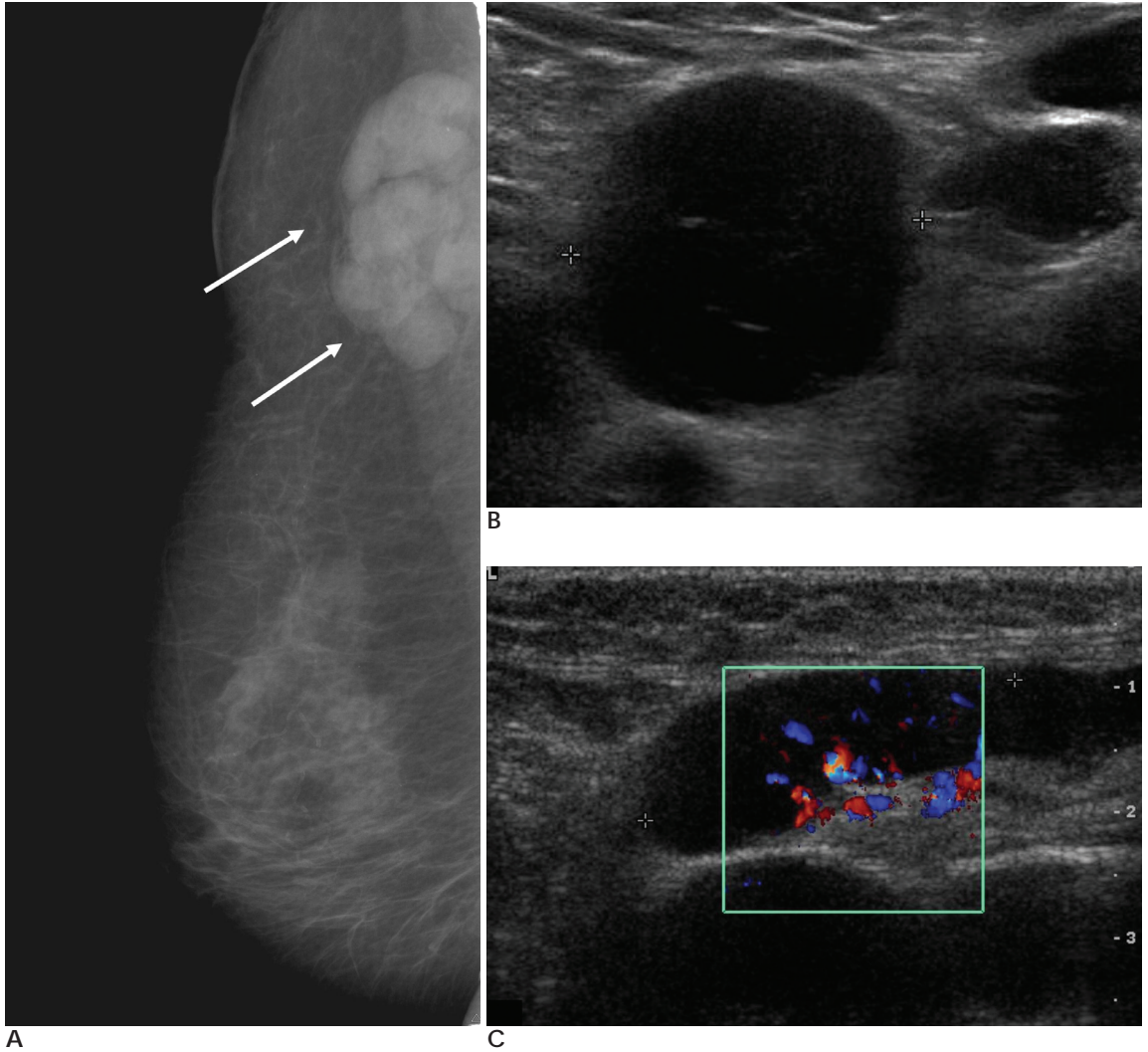
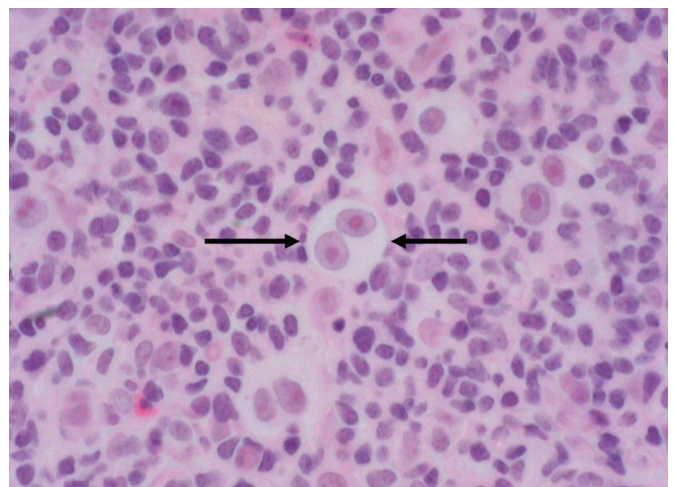


**Fig. 5.** Primary Hodgkin's lymphoma in an 85-year-old female with a palpable right axillary mass.

**A.** Mammography shows hyperdense mass in right axilla (arrows).

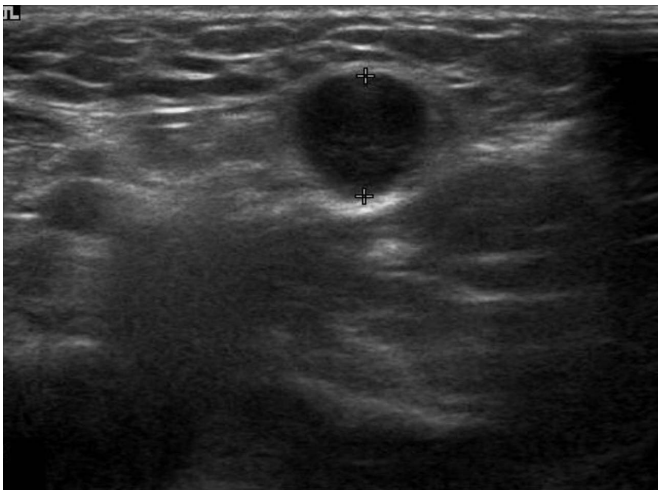
**B, C.** Ultrasonography shows multiple enlarged conglomerated lymph nodes without central fatty hila. The color doppler scan shows diffuse hypervascularities in the central and peripheral portions of lymph nodes.

**D.** Sonography-guided core biopsy was performed for the right axillary mass. Photomicrograph shows Reed-Sternberg cells (arrows) in Hodgkin's lymphoma (x400, H-E stain) and CD30 positive immunoreactivity in the Hodgkin's lymphoma (CD30 immunostaining, not shown).

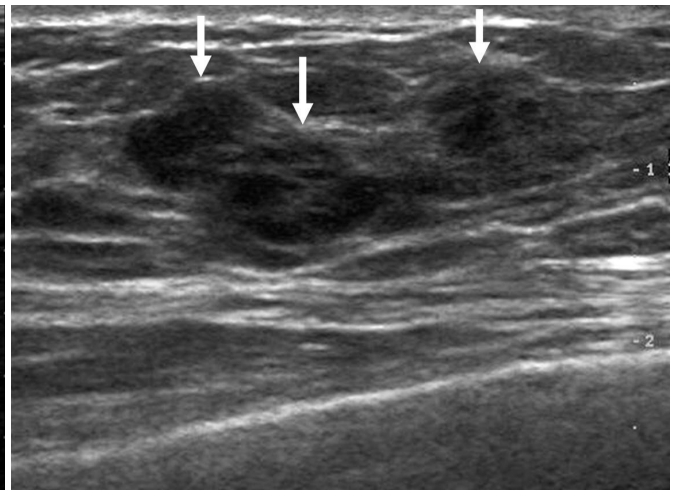


**D**

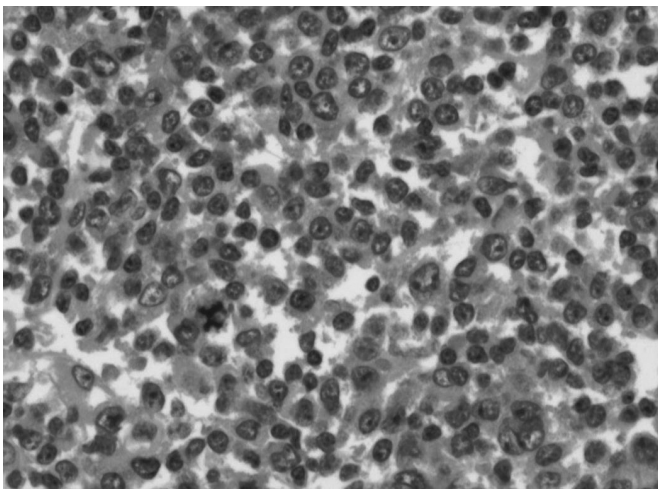
가 (6). 가 (7) (Fig. 5, 6). (claw sign)가 (7) (Fig. 7). (Hemangioma) (perilobular type), (cavernous type) (capillary type) (perilobular type) 2 mm 가 4 mm 2 cm (cavernous type) (capillary type) 가 (stratified squamous epithelium) 가



A



B



C

**Fig. 6.** Secondary Non-Hodgkin's lymphoma in a 46-year-old female with masses in the right axilla and right breast. This patient has multiple lymphomas in the bilateral ovaries and cervical lymph nodes.  
**A.** Ultrasonography of the right axilla reveals several round hypervascular lymph nodes without central fatty hila.  
**B.** Ultrasonography of the right breast shows several indistinct margined heterogeneously hypoechoic nodules with peritumoral hyperechoic halo (arrows) and ductal extensions in the right upper outer quadrant.  
**C.** Sonography-guided core biopsies were performed for the right axillary and breast masses. Photomicrograph shows diffuse infiltration of large atypical lymphoid cells (Diffuse large B cell lymphoma) (H-E stain,  $\times 400$ ).

가 (phlebolith)

가 8). (low grade angiosarcoma)

(Kaposi's sarcoma)

(vascular pole)

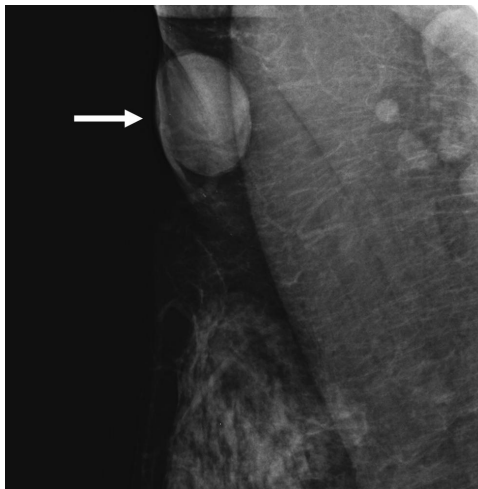
가 (9), MRI T2

가

가

가 1 cm

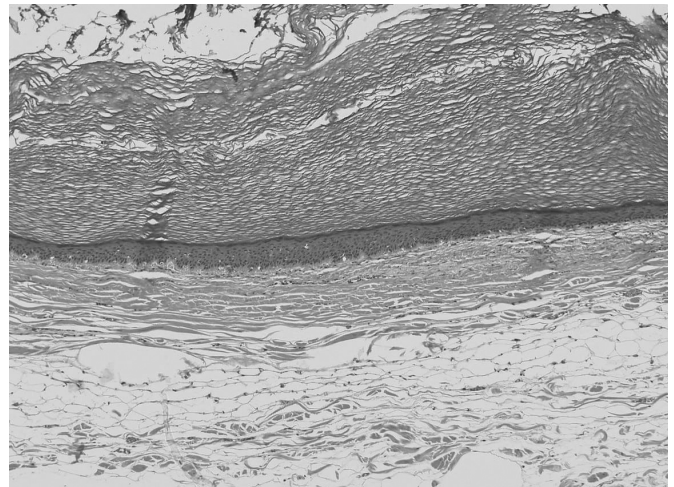
5-6 (milk line or milk



A



B



C

**Fig. 7.** Epidermal inclusion cyst in a 37-year-old female at the right axilla **(A)** A circumscribed ovoid mass with skin thickening (arrows) was noted on the mammography. **B.** Ultrasonography shows circumscribed oval shaped heterogeneous echogenic mass in the right axilla with skin thickening in the subcutaneous fat layer and adjacent dermis. This mass is in front of the anterior layer of superficial fascia. **C.** An excisional biopsy of the right axillary mass was performed. Photomicrograph shows a cyst lined by stratified squamous epithelium (× 100, H-E stain).



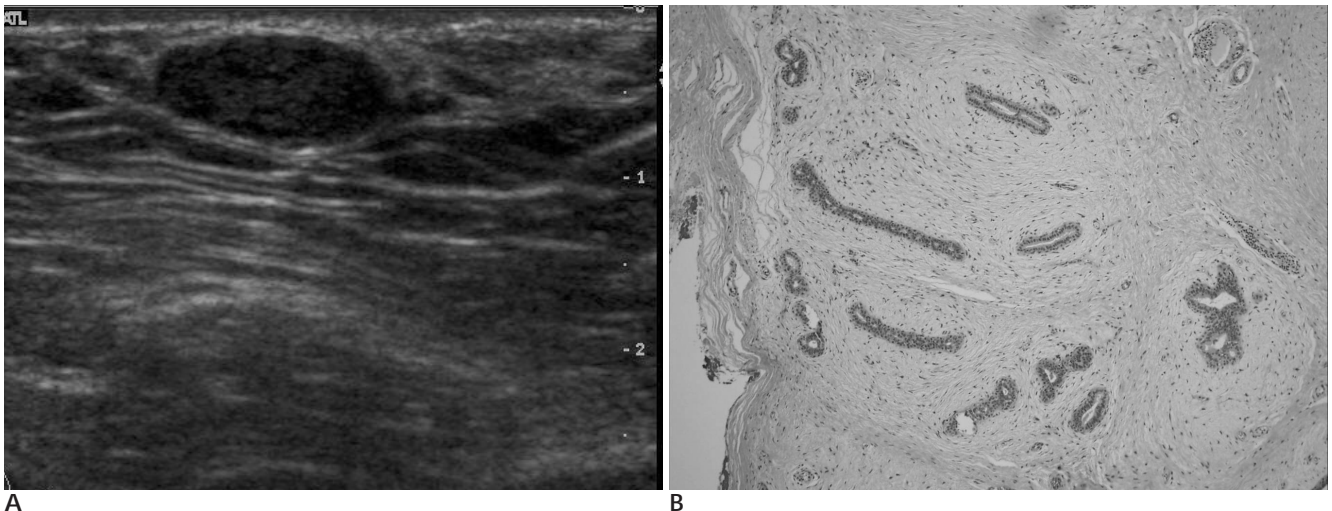


**Fig. 9.** Fibroadenoma in a 53-year-old female at the right axilla. **A.** Ultrasonography shows an ovoid circumscribed hypoechoic nodule in the right accessory breast. **B.** An excisional biopsy was performed for the axillary mass. Photomicrograph shows a sharply demarcated mass with intracanalicular growth pattern of fibroadenoma ( $\times 100$ , H-E stain).

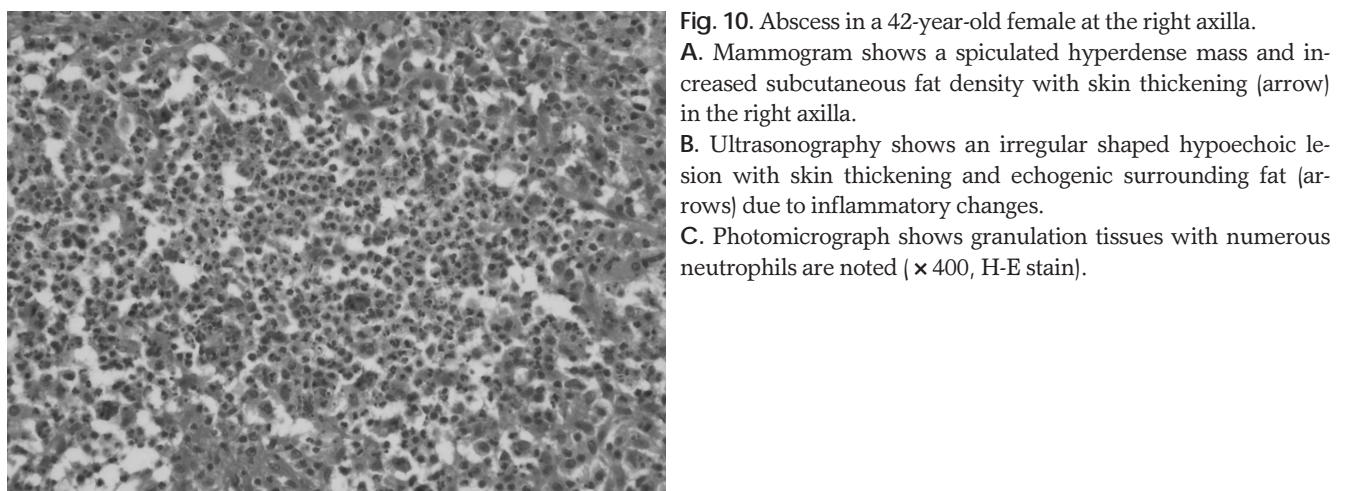
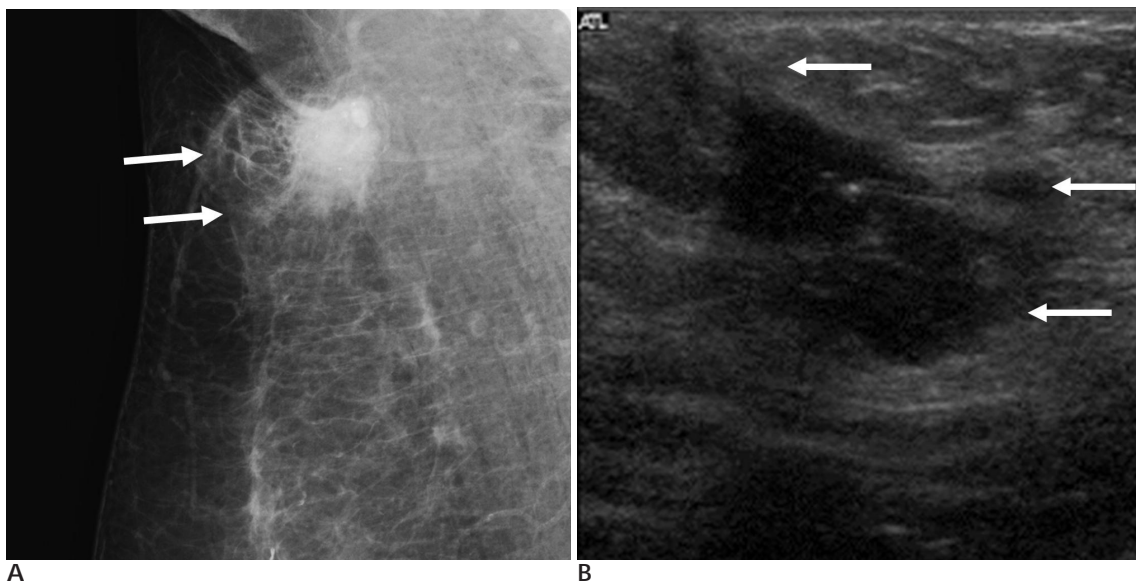


**Fig. 10.** Abscess in a 42-year-old female at the right axilla. **A.** Mammogram shows a spiculated hyperdense mass and increased subcutaneous fat density with skin thickening (arrow) in the right axilla. **B.** Ultrasonography shows an irregular shaped hypoechoic lesion with skin thickening and echogenic surrounding fat (arrows) due to inflammatory changes. **C.** Photomicrograph shows granulation tissues with numerous neutrophils are noted ( $\times 400$ , H-E stain).

C

(Fig. 9)

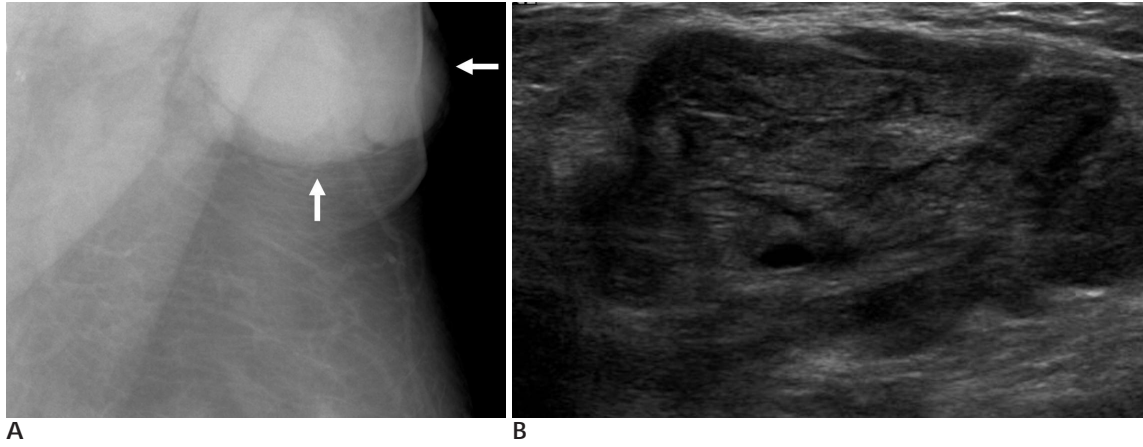
(Abscess)

(mammary duct)

(Staphylococcus aureus)

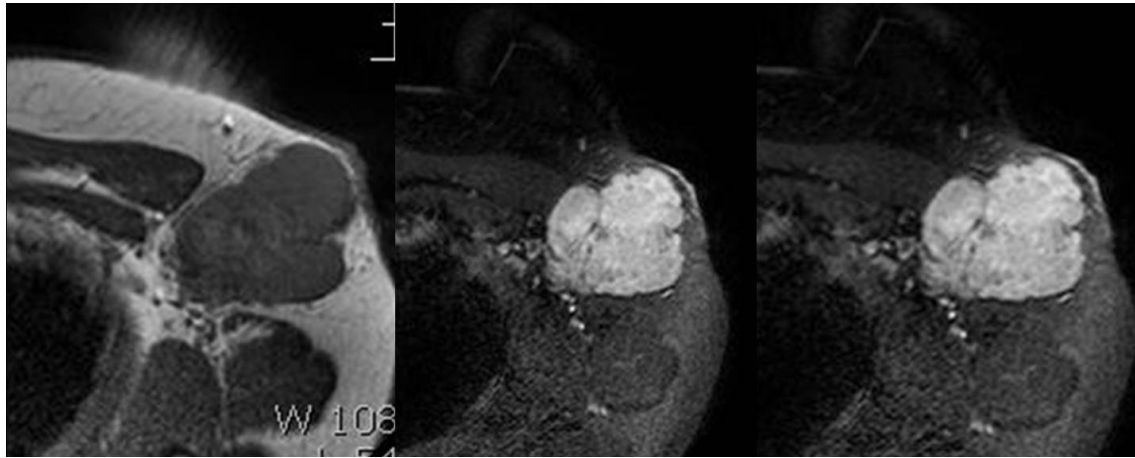
(Streptococcus)

(Fig. 10).

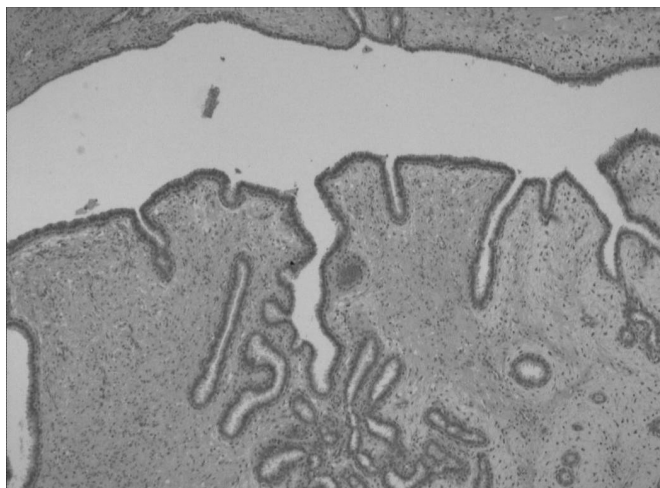


A

B



C



D

**Fig. 11.** Phyllodes tumor in a 33-year-old female at the left axillary accessory breast.

**A.** Mammography shows huge circumscribed hyperdense mass in the left axilla.

**B.** Ultrasonography shows large lobulated solid mass containing central hypoechoic linear cystic septae.

**C.** MRI shows a large axillary mass with central septations, showing heterogeneously low signal intensity on T1weighted image (left), high signal intensity on the fat-suppressed T2 weighted image (center). Gadolinium-enhanced dynamic MR shows a diffusely enhanced axillary mass with non-enhanced central septae (right). The time/signal intensity curve revealed a rapid-raise and plateau pattern (not shown).

**D.** An excisional biopsy was performed for the left axillary mass. Photomicrograph shows leaf-like processes lined by bland epithelium with hypercellular stroma without atypia and mitotic activity ( $\times 100$ , H-E stain).

(Phyllodes Tumor)

가 가  
(cleft)

가 25% , 가 10%

가

가

. MR 가

가  
(10) (Fig. 11).

1. Vassallo P, Edel G, Roos N, Naguib A, Peters PE. In-vitro high-resolution ultrasonography of benign and malignant lymph nodes. A sonographic-pathologic correlation. *Invest Radiol* 1993;28:698-705
2. Leibman AJ, Wong R. Findings of mammography in the axilla. *AJR Am J Roentgenol* 1997;169:1385-1390
3. Muttarak M, Pojchamarnwiputh S, Chaiwun B. Mammographic features of tuberculous axillary lymphadenitis. *Australas Radiol* 2002;46:260-263
4. Madle-Samardzija N, Turkulov V, Vukadinov J, Stajnic S, Canak G. Histiocytic necrotizing lymphadenitis (Kikuchi-Fujimoto disease). *Med Pregl* 2000;53:513-516
5. Murphy TJ, Mowad CM, Feig SA, Nussbaum SA, Hyland JC. Breast imaging case of the day. Dermatopathic lymphadenopathy. *Radiographics* 1998;18:536-539
6. Steinkamp HJ, Mueffelman M, Bock JC, Thiel T, Kenzel P, Felix R. Differential diagnosis of lymph node lesions: a semiquantitative approach with Color Doppler Ultrasound. *Br J Radiol* 1998;71:828-833
7. Appelbaum AH, Evans GF, Levy KR, Amirkhan RH, Schumpert TD. Mammographic Appearances of Male Breast Disease. *Radiographics* 1999;19:559-568
8. Stavros AT. *Breast Ultrasound*. 1st ed, Philadelphia, Lippincott Williams & Wilkins 2004:435-439
9. Glazebrook KN, Morton MJ, Reynolds C. Vascular Tumors of the Breast: Mammographic, Sonographic, and MRI Appearances. *AJR Am J Roentgenol* 2005;184:331-338
10. Wurdinger S, Herzog AB, Fischer DR, Marx C, Raabe G, Schneider A, et al. Differentiation of phyllodes breast tumors from fibroadenomas on MRI. *AJR Am J Roentgenol* 2005;185:1317-1321

## Spectrum of Axillary Disorders (Excluding Metastasis from Breast Cancer): Radiological and Pathological Correlation: A Pictorial Essay<sup>1</sup>

Ho Jun Kim, M.D., Keum Won Kim, M.D., Yong Sung Park, M.D., Dong Jin Chung, M.D.,  
Young Jun Cho, M.D., Cheol Mog Hwang, M.D., Hyeun Mi Yoo, M.D.,  
Yoon Mee Kim, M.D.<sup>2</sup>, Mee Ran Lee, M.D.<sup>3</sup>

<sup>1</sup>Department of Radiology, Konyang University Hospital

<sup>2</sup>Department of Pathology, Konyang University Hospital

<sup>3</sup>Department of Radiology, Eulji University Hospital

Axillary disorders originate from an axillary lymph node, subcutaneous fat layer, accessory breast, nerve, vessel and muscle. The most common causes of a palpable axillary mass are a lymph node pathology containing a benign axillary lymphadenopathy, and malignant lymph nodes such as a metastatic lymphadenopathy from breast cancer and a malignant lymphoma. For the detection of masses in the axilla, mammography and sonography are the imaging modalities of choice. We present a spectrum of various axillary masses with correlative radiological imaging and pathological findings in this pictorial essay. Knowledge of the radiological findings of various axillary disorders is useful for a differential diagnosis and for preventing unnecessary invasive procedures.

**Index words :** Radiography

Ultrasonography

Mammary neoplasms

Lymphatic system

Lymphatic metastasis

Axilla

Address reprint requests to : Keum Won Kim, M.D., Department of Radiology, Konyang University Hospital,  
685, Gasoowon-dong, Seo-gu, Daejeon 302-718, Korea  
Tel. 82-42-600-9222 Fax. 82-42-600-9193 E-mail : lizkim1@hanmail.net